Measurement of persistence in 1-D diffusion

Glenn P. Wong, Ross W. Mair, and Ronald L. Walsworth
Harvard-Smithsonian Center for Astrophysics, 60 Garden St., Cambridge, MA 02138

David G. Cory
Department of Nuclear Engineering, Massachusetts Institute of Technology, Cambridge, MA 02139
(September 2, 2000)

Using a novel NMR scheme we observed persistence in 1-D gas diffusion. Analytical approximations and numerical simulations have shown that for an initially random array of spins undergoing diffusion, the probability $p(t)$ that the average spin orientation in a given region has not changed sign (i.e., "persists") up to time t follows a power law $t^{-\theta}$, where θ depends on the dimensionality of the system. The large nuclear spin polarization of laser-polarized ^{129}Xe gas allowed us both to prepare an initial "quasi-random" 1-D array of spin orientations and then to perform real-time NMR imaging to monitor the spin diffusion. Our measurements are consistent with theoretical and numerical predictions of $\theta \approx 0.12$. We also observed finite size effects for long time gas diffusion.

02.50.-r,05.40.-a,05.70.Ln,82.20.Mj,76.60.Pc

The dynamics of non-equilibrium systems is a field of great current interest, including such topics as phase ordering in binary alloys, uniaxial ferromagnets, and nematic liquid crystals, as well as coarsening of soap froth and diffusion of inhomogeneous fluids (*e.g.* [1]). The evolving spatio-temporal structures in these non-equilibrium systems depend crucially on the history of the system's evolution and are not completely characterized by simple measures such as two-time correlation functions, which do not give information on the entire system history. Therefore, an important problem in the study of non-equilibrium dynamics is the development of simple and easily measurable quantities that give non-trivial information about the history of the system's evolution. The recently identified phenomenon of "persistence" is such a quantity: it characterizes the statistics of first passage events in spatially extended non-equilibrium systems [2–15]. Practically, persistence may be important in determining what fraction of a system has reached a threshold condition as a function of time; for example, in certain chemical reactions or disinfectant procedures.

Consider a non-equilibrium scalar field $\phi(\mathbf{x}, t)$ fluctuating in space and time according to some dynamics (e.g., a random array of interdiffusing spins). Persistence is the probability $p(t)$ that at a fixed point in space the quantity $\mathrm{sgn}[\phi(\mathbf{x}, t) - \langle\phi(\mathbf{x}, t)\rangle]$ has not changed sign up to time t. It has been found that this probability decays as a power law $p(t) \sim t^{-\theta}$, where the persistence exponent θ is generally nontrivial. This exponent depends both on the system dimensionality and the prevalent dynamics, and is difficult to determine analytically due to the non-Markovian nature of the phenomena. Although θ has been calculated – largely using numerical techniques – for such systems as simple diffusion [3–5], the Ising model [2,8,11], and the more generalized q-state Potts model [2,12], few measurements of persistence have been performed (see Table I). In particular, "breath figures" [13], 2-D soap froth [14], and twisted nematic liquid crystals [15] are the only systems for which experimental results have been reported.

TABLE I. A sample of reported persistence exponents. All values except those indicated are derived from numerical simulations; (*) denotes exact analytical results, (†) experimental measurements, and (‡) the result reported here.

Dim.	**Diffusion**	**Ising**	**q-Potts**
1	0.12, **0.118**‡	3/8*, 0.35	$-\frac{1}{8} + \frac{2}{\pi^2}\left[\cos^{-1}\left(\frac{(2-q)}{\sqrt{2q}}\right)\right]^{2}{}^*$
2	0.19	0.22, 0.19†	0.86, 0.88† (large q)
3	0.24	0.26	
refs	*[3–5]*	*[2,11] [15]*†	*[2,12] [14]*†

In this paper we present the first measurement of persistence in a system undergoing diffusion. Our experiment is also the first to observe persistence in one dimension (1-D). We employed a novel NMR technique to create a "quasi-random" initial spatial variation in the spin orientation of a sample of laser-polarized ^{129}Xe gas. Subsequent 1-D NMR imaging, repeated at different times, allowed us to monitor the temporal evolution of the ensemble and observe persistence from the fraction of 1-D regions in the sample that did not change their spin orientation as a function of time. Using a simple theory (the "independent interval approximation") and numerical simulations, both Majumdar *et al.* [3] and Derrida *et al.* [4] independently found that $\theta \approx 0.121$ for 1-D diffusion. Newman and Toroczkai [5] found $\theta \approx 0.125$ in 1-D using an analytic expression for the diffusion persistence exponent. Our measurements are consistent with these calculations.

Recently, laser-polarized noble gas NMR has found wide application in both the physical and biomedical sciences. Examples include fundamental symmetry tests [16], probing the structure of porous media [17], and imaging of the lung gas space [18]. These varied investigations, as well as the experiment reported here, exploit

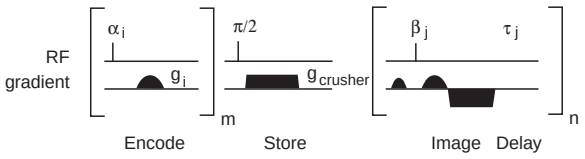

FIG. 1. NMR pulse sequence used to encode a 1-D "quasi-random" pattern on the average spin orientation of laser-polarized ^{129}Xe gas. Temporal evolution of the magnetization pattern is monitored with n repetitions of a 1-D FLASH imaging routine. For example, with $m = 8$ encoding RF pulse/gradient pairs, the encoding pulse angles α_i = [30°, 35°, 37°, 41°, 45°, 50°, 63.5°, and 90°] while the gradient amplitudes g_i were chosen randomly. The imaging pulse angle β_j was fixed at 8°and the diffusion times τ_j were varied from 2.4 ms up to $\sim$ 2 seconds. The encoding, crusher, pre-image crusher, and imaging wind and rewind gradients were pulsed for 1, 20, 3, 2, and 2.56 ms, respectively. The maximum gradient available was 6.7 G/cm.

special features of laser-polarized noble gas: the large nuclear spin polarization ($\sim$ 10%) that can be achieved with optical pumping techniques; the long-lived nuclear spin polarization of the spin-1/2 noble gases ^{129}Xe and ^{3}He; and rapid gas-phase diffusion.

We performed laser-polarization of xenon gas using spin-exchange optical pumping [19]. We filled a coated cylindrical glass cell [20] ($\sim$ 9 cm long, 2 cm I.D.) with approximately 3 bar of xenon gas isotopically enriched to 90% ^{129}Xe, 400 torr of N_2 gas, and a small amount of Rb metal. We heated the sealed cell to $\sim$ 100°C to create a significant Rb vapor using a resistively-heated oven situated in the fringe field (0.01 Tesla) of a high field magnet. Optical pumping on the Rb D1 line was achieved with 15 W of circularly-polarized 795 nm light (FWHM $\sim$ 3 nm) from a fiber-coupled laser diode array. After 20 minutes the ^{129}Xe gas was routinely nuclear spin-polarized to 1% by spin-exchange collisions with the Rb vapor. We next cooled the cell to room temperature in a water bath – effectively condensing the Rb vapor – and placed the cell inside a homemade RF solenoid coil (2.5 cm diameter, 15 cm long, $Q \sim 900$) centered in a 4.7 T horizontal bore magnet (GE Omega/CSI spectrometer/imager) with ^{129}Xe Larmor frequency = 55.345 MHz. To allow the gas temperature to reach equilibrium, we left the cell in place for 20 minutes before starting the persistence measurements. Under these conditions the ^{129}Xe polarization decay time constant (T_1) was in excess of 3 hours, with a ^{129}Xe diffusion coefficient of 0.0198 cm^2/s [21].

The NMR pulse sequence we used to observe persistence in laser-polarized ^{129}Xe gas diffusion is shown schematically in Fig. 1. The initial portion of the pulse sequence encodes a 1-D "quasi-random" pattern on the average spin orientation of the laser-polarized ^{129}Xe gas sample. The pattern is quasi-random in that there must be a minimum length scale to the induced variations in the ^{129}Xe magnetization (typically 500 μm) for there to be sufficient NMR signal for useful imaging. Nevertheless, at longer length scales the induced pattern must be random enough that persistence behavior can be expected. Ideally, $\langle\phi(x,0)\phi(x',0)\rangle = \delta(x-x')$; however, calculations indicate that it is sufficient for the initial condition correlator to decrease faster than $|x-x'|^{-1}$ [3].

The quasi-random patterning pulse sequence employs "cumulative k-space encoding." Recall that one can describe an NMR experiment in terms of a reciprocal or k-space formalism [22], where k is the wave number characterizing a magnetization modulation or "grating" created by RF and magnetic field gradient pulses. One can represent a spatial magnetization distribution along a fixed axis by a combination of three basis functions: $\sin(kx)$ for variations in the longitudinal magnetization M_z, and $e^{\pm ikx}$ for positive and negative "helices" of transverse magnetization $M_{x,y}$. RF pulses effectively mix the components of the magnetization (with amplitudes determined by the flip angle) [23] and gradient pulses change the k values of the transverse magnetization [22]. By using m pairs of varying RF and random-strength gradient pulses in rapid succession it is possible to create a complex and near-random spatial magnetization distribution; i.e., a large number of gratings with different k-values and amplitudes are superposed. As Nelson and coworkers showed [24], the maximum number $N_{max}(m)$ of k values one can expect from m pairs of RF and gradient pulses is given by

$$N_{max}(m) = \frac{1}{4}(3^m - 2m - 1). \quad (1)$$

We found that six to eight RF/gradient pulse pairs (m = 6–8) were optimal for the desired quasi-random 1-D patterning of the ^{129}Xe spin orientation. $m < 6$ resulted in a pattern that was not sufficiently random, while $m > 8$ significantly reduced the signal-to-noise ratio (SNR) of the NMR images. The requirement of $m \geq 6$ is supported by numerical calculations in which we modeled the NMR encoding sequence and simulated the subsequent gas diffusion using a finite difference first-order forward Euler scheme [4,25]: we found persistence behavior (i.e., $p(t) \sim t^{-\theta}$) only when $m \geq 6$. Furthermore, we acquired 512 (time domain) data points for each image. The number of data points per image was limited by the available NMR signal (i.e., the ^{129}Xe polarization), the necessity of rapid data acquisition to avoid excessive diffusion during the imaging sequence itself, and the maximum imaging gradient strength available. Since there is a one-to-one mapping between the time domain and k-space, we could discern at most 512 magnetization gratings with different k values. For $m = 6, 7, 8$, $N_{max}(m) = 179, 543$, and 1636, respectively. Hence, 7 or more RF/gradient pulses maximally covered the avail-

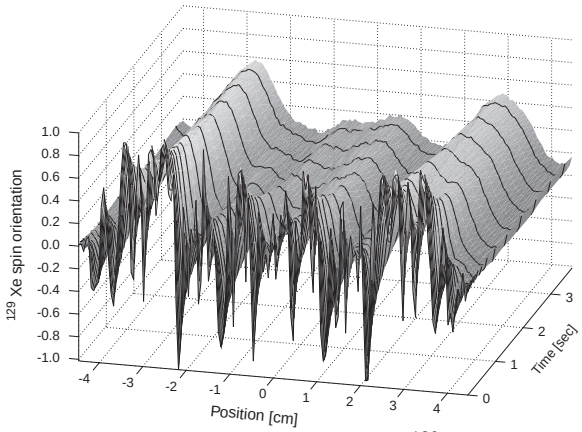

FIG. 2. Typical set of 1-D images of ^{129}Xe spin orientation from a single experimental run. For this example, 8 encoding RF pulse/gradient pairs were used to create an initial quasi-random pattern of ^{129}Xe spin orientation on length scales $\geq 500\mu$m. 32 images were acquired at logarithmically increasing times. Contours from every other image are overlayed on the surface plot, which includes all 32 images.

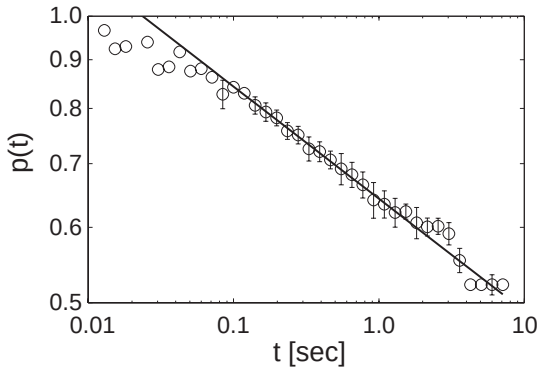

FIG. 3. A log-log plot of $p(t)$, the fraction of spin orientation regions that had not changed sign up to a time t, representing the sum of ~ 30 different experimental runs. The solid line is a weighted linear least-squares fit to the data for 0.1 s $< t <$ 1 s, and yields $\theta = 0.118 \pm 0.008$. Error bars are derived from the number of pixels with amplitudes close to the image noise level and are shown when they exceed the plot symbol diameter.

able k-space and produced as random a 1-D spatial distribution of the ^{129}Xe magnetization as was detectable (given the constraints of finite sample length and minimum length scale of variations $\sim$ 500 μm). The fact that our simulations (and data, see below) yield persistence behavior for $m = 6$ indicates some robustness with respect to initial conditions.

After the pattern encoding part of the NMR pulse sequence, a $\pi/2$ RF pulse "stores" the quasi-random magnetization distribution along the longitudinal (z) direction while a subsequent strong (crusher) gradient pulse dephases any remaining transverse magnetization. The quasi-random magnetization distribution then evolves with time due to diffusion and is monitored by a series of 1-D FLASH (Fast Low Angle SHot) NMR images [26] (see Fig. 1). We used a field of view (FOV) of 31.5 cm with 0.6 mm resolution, which thus divided the 9 cm cell into about 150 discernible spatial regions. We typically employed 8° excitation RF flip angles and acquired 32 1-D images spaced logarithmically in time from $\sim$ 3 ms to 5 s for a single experimental run. An example of the images acquired in one such run are shown in Fig. 2. We derived spin orientations (aligned or anti-aligned to the main magnetic field) from the phase information contained in the time-domain NMR image data and spatial positions from the frequency information [27]. Each experimental run thus provided a record of the ^{129}Xe gas spin orientation as a function of position and time proceeding from the initial quasi-random pattern to the equilibrium condition of homogeneous (near-zero) polarization.

To measure persistence, we noted the sign of the ^{129}Xe spin orientation in each spatial region (i.e., in each 1-D image pixel) and counted how many remained unchanged as a function of time. We equated the probability $p(t)$ with the fraction of pixels that had not changed sign up to time t. We chose $t = 0$ to coincide with the first image and assigned the time index for each image to be the start time of the imaging RF pulse. Images with SNR < 40 were excluded from the data to minimize uncertainty in pixel sign changes. We conducted about 30 experiments with image SNR > 40, each with a unique set of randomly chosen encoding gradients $\{g_i\}$. We employed two averaging schemes to combine the results from different experimental runs. In the first method, we used a linear least-squares fit of $\log[p(t)]$ vs. $\log[t]$ for each run, resulting in a distribution of power law exponents with a weighted mean $\theta = 0.119 \pm 0.048$. With our numerical simulations of cumulative k-space-encoded initial conditions, we found that this averaging scheme results in a gaussian distribution of exponents with a mean value $\theta \approx 0.12$ in agreement with previous calculations for 1-D diffusion [3–5] and our experimental results. In the second averaging scheme, we combined the data from all experimental runs; hence $p(t)$ represented the fraction of total pixels from all experiments that had not changed sign up to time t. We found $p(t) \sim t^{-\theta}$ with $\theta = 0.118 \pm 0.008$ for 0.1 s $< t <$ 1 s. Figure 3 shows a log-log plot of $p(t)$ vs. t when the data is averaged using this method.

The observed deviations from power law behavior for $t <$ 0.1 s and $t >$ 1 s are explained by resolution and finite size effects, respectively. At short times persistence is not observed because ^{129}Xe atoms have not yet diffused across a single spin orientation region $\delta x \approx 500\mu$m. The relevant diffusion time is $(\delta x)^2/(2D_{Xe}) \approx 0.1$ s. At long times, the pattern of ^{129}Xe spin orientation becomes

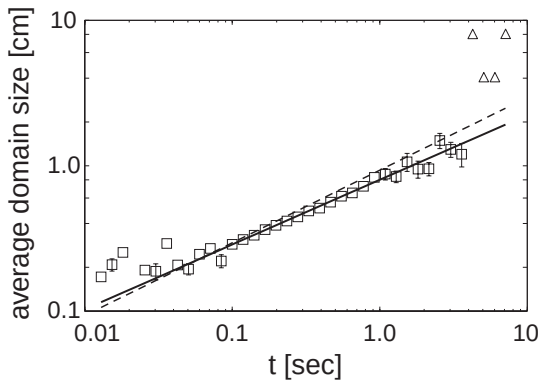

FIG. 4. The average spin orientation domain size L as a function of time t, derived from all experimental runs. For 0.1 s $< t <$ 1 s, $L \sim t^{\alpha}$ where $\alpha = 0.45 \pm 0.02$ (solid line). The dotted line shows the expected $L \sim t^{1/2}$ behavior for an infinite system. The error in L is shown where it exceeds the plot symbol size. The finite size limit on L is evident in the four late-time points ($\triangle$), which were taken from the only two runs with sufficient SNR at long times.

ordered on length scales comparable to the sample dimension, thus curtailing the rate of sign-changing. Both the short and long time deviations are also seen in Fig. 4, where the average length L of spin orientation domains from all experimental runs is plotted against time. For 0.1 s $< t <$ 1 s, our data are in reasonable agreement with the expected power law $L \sim t^{1/2}$ for diffusion. However, at short times L is near the limit to image resolution while at longer times L grows more rapidly as it approaches the dimension of the sample cell.

In conclusion, we experimentally measured a persistence exponent $\theta \approx 0.12$ for 1-D diffusion, consistent with analytical and numerical studies. We performed the measurement using a novel NMR scheme with laser-polarized ^{129}Xe gas which allowed us to both encode a "quasi-random" spatial pattern of spin orientation and monitor its evolution over several seconds. We also observed the effect of finite sample size for long time diffusion. In future work the experimental technique employed in this study may allow measurements of persistence in 2 and 3-D diffusion, in heterogeneous systems (e.g., porous media) infused with noble gas, and in 'patterns' [28].

The authors thank Satya Majumdar, Michael Cressimano, and Lukasz Zielinski for useful discussions. This work was supported by NSF Grant No. CTS-9980194, NASA Grant No. NAG9-1166, and the Smithsonian Institution Scholarly Studies Program.

[1] A. J. Bray, Adv. Phys. **32**, 357 (1994).
[2] B. Derrida, V. Hakim, and V. Pasquier, Phys. Rev. Lett. **75**, 751 (1995).
[3] S. N. Majumdar, C. Sire, A. J. Bray, and S. J. Cornell, Phys. Rev. Lett. **77**, 2867 (1996).
[4] B. Derrida, V. Hakim, and R. Zeitak, Phys. Rev. Lett. **77**, 2871 (1996).
[5] T. J. Newman and Z. Toroczkai, Phys. Rev. E **58**, R2685 (1998).
[6] B. P. Lee and A. D. Rutenberg, Phys. Rev. Lett. **79**, 4842 (1997).
[7] J. Krug, H. Kallabis, S. N. Majumdar, S. J. Cornell, A. J. Bray, and C. Sire, Phys. Rev. E **56**, 2702 (1997).
[8] S. Jain, Phys. Rev. E **60**, R2445 (1999).
[9] C. Sire, S. N. Majumdar, and A. Rüdinger, Phys. Rev. E **60**, 1258 (2000).
[10] V. M. Kendon, M. E. Cates, and J.-C. Desplat, Phys. Rev. E **61**, 4029 (2000).
[11] S. N. Majumdar and C. Sire, Phys. Rev. Lett. **77**, 1420 (1996).
[12] B. Derrida, P. M. C. de Oliveira, and D. Stauffer, Physica A **224**, 604 (1996).
[13] M. Marcos-Martin, D. Beysens, J. P. Bouchaud, C. Godrèche, and I. Yekutieli, Physica A **214**, 396 (1995).
[14] W. Y. Tam, R. Zeitak, K. Y. Szeto, and J. Stavans, Phys. Rev. Lett. **78**, 1588 (1997).
[15] B. Yurke, A. N. Pargellis, S. N. Majumdar, and C. Sire, Phys. Rev. E **56**, R40 (1997).
[16] D. Bear, T. E. Chupp, K. Cooper, S. DeDeo, M. Rosenberry, R. E. Stoner, and R. L. Walsworth, Phys. Rev. A **57**, 5006 (1998).
[17] R. W. Mair, G. P. Wong, D. Hoffmann, M. D. Hürlimann, S. Patz, L. M. Schwartz, and R. L. Walsworth, Phys. Rev. Lett. **83**, 3324 (1999).
[18] M. S. Albert, G. D. Cates, B. Driehuys, W. Happer, B. Saam, C. S. Springer, Jr., and A. Wishnia, Nature **370**, 199 (1994).
[19] T. G. Walker and W. Happer, Rev. Mod. Phys. **69**, 629 (1997).
[20] We used a wall coating of octadecyltrichlorosilane (OTS) to reduce Xe-wall interactions and hence increase longitundinal relaxation times.
[21] R. W. Mair, D. G. Cory, S. Peled, C.-H. Tseng, S. Patz, and R. L. Walsworth, J. Mag. Res. **135**, 478 (1998).
[22] A. Sodickson and D. G. Cory, Prog. Nucl. Magn. Res. Spec. **33**, 77 (1998).
[23] J. Hennig, J. Mag. Res. **78**, 397 (1988).
[24] R. I. Nelson, Y. Maguire, D. F. Caputo, G. Leu, Y. Kang, M. Pravia, D. Tuch, Y. S. Weinstein, and D. G. Cory, Concepts. in. Magn. Res. **10**, 331 (1998).
[25] W. H. Press, B. P. Flannery, S. A. Teukolsky, and W. T. Vetterling, *Numerical Recipes in C* (Cambridge University Press, Cambridge, U.K., 1988).
[26] A. Haase, J. Frahm, D. Matthaei, W. Hänicke, and K.-D. Merboldt, J. Mag. Res. **67**, 258 (1986).
[27] C. B. Ahn and Z. H. Cho, IEEE Trans. Med. Imag. **MI-6**, 32 (1987).
[28] S. N. Majumdar, Curr. Sci. **77**, 370 (1999).